2012

Multi-objective Optimization of Sustainable Single-Effect Water/Lithium Bromide Absorption Cycle

B. H. Gebreslassie
Purdue University

E. A. Groll
Purdue University

S V. Garimella
Purdue University, sureshg@purdue.edu

Gebreslassie, B. H.; Groll, E. A.; and Garimella, S V., "Multi-objective Optimization of Sustainable Single-Effect Water/Lithium Bromide Absorption Cycle" (2012). *CTRC Research Publications.* Paper 177.
http://dx.doi.org/10.1016/j.renene.2012.03.023

Multi-objective optimization of sustainable single-effect water/Lithium Bromide absorption cycle

Berhane H. Gebreslassie[a,b], Eckhard A. Groll[a,b], Suresh V. Garimella[a,*]

[a]*Cooling Technologies Research Center, School of Mechanical Engineering, Purdue University*

585 Purdue Mall, West Lafayette, IN 47907-2088, USA

[b]*Herrick Laboratories, School of Mechanical Engineering, Purdue University*

140 S. Martin Jischke Drive, West Lafayette, IN 47907-2031, USA

Abstract

A rigorous mathematical approach is developed for optimization of sustainable single-effect water/Lithium Bromide (LiBr) absorption cooling cycles. The multi-objective formulation accounts for minimization of the chiller area as well as the environmental impact associated with the operation of the absorption cycle. The environmental impact is quantified based on the global warming potential and the Eco-indicator 99, both of which follow principles of life cycle assessment. The design task is formulated as a bi-criterion non-linear programming problem, the solution of which is defined by a set of Pareto points that represent the optimal compromise between the total area of the chiller and global warming potential. These Pareto sets are obtained via the epsilon constraint method. A set of design alternatives are provided for the absorption cycles rather than a single design; the best design can be chosen from this set based on the major constraints and benefits in a given application. The proposed approach is illustrated design of a typical absorption cooling cycle.

Keywords: Absorption cycle, Multi-objective optimization, life cycle assessment, Global warming potential, Eco-indicator 99, water/lithium bromide

---

[*]*Corresponding author*

Email address: sureshg@purdue.edu *(Suresh V. Garimella)*

1. Introduction

According to the Intergovernmental Panel on Climate Change (IPCC), global GHG emissions increased by 70% between 1970 and 2004 [1], growing from 28.7 to 49 Gigatonnes of carbon dioxide equivalent ($GtCO_{2\text{-}eq}$). The International Energy Agency reported that 65 % of all

greenhouse gas emissions in 2009 were related to energy use of some kind [2]. As an example, to meet a target $CO_{2\text{-}eq}$ concentration of 450 ppm in the year 2020, the United States must reduce its CO_2 emissions by 16 % from the building sector and by 25% from the power generation sector relative to 2007 values, in addition to reductions from other emissions sources [2]. Therefore, steps toward climate change mitigation must focus on significantly decarbonizing energy technologies. Environmentally friendly and energy-efficient technologies must be promoted so that the environmental impact of the cooling and heating needs in the building sector is minimized without significant economic cost.

Absorption cycles are gaining in popularity for air conditioning systems because of benefits to both the environment and energy consumption. However, the large number of heat exchange units required to accommodate the absorption and desorption processes of the refrigerant results in an increase in the investment cost, posing a challenge to the implementation of such systems. These costs can be reduced through system optimization strategies, such as those developed in the present work, positioning the absorption chillers as a real alternative to conventional cooling cycles in the market.

Absorption cycles are typically optimized either component by component or variable by variable. The most widely used approach is thermoeconomic optimization which merges exergy and economic analysis. Kizilkan et al. [3] optimized the single-effect water/LiBr absorption cycle based on the structural method of Bayer as described in [4]. The main units were considered independently and linked through coefficients of structural bonds to optimize the whole cycle. Gebreslassie et al. [5] also followed a similar approach for the optimal design of the single-effect ammonia/water absorption cycle. However, this approach assesses only a subset of the possible design solutions. That is, in optimizing each unit of the cycle independently, the efficiency-related variable of the unit (such as the minimum temperature approach of the heat exchanger) is allowed to vary while the variable for other units of the cycle is held constant.

It is important that a modeling approach be developed that can facilitate the generation and evaluation of the full set of possible design alternatives for absorption cycles. While rigorous mathematical optimization approaches have been applied widely in design optimization of other industrial processes [6, 7], such approaches have not seen widespread application in the design of cooling systems; recently, optimization of ammonia/water absorption cycles has been reported [8-10]. The design task is posed as an optimization problem and solved using

standard techniques for linear, nonlinear, mixed integer linear and mixed integer nonlinear (LP, NLP, MILP, MINLP, respectively) problems.

While these studies focused on optimizing the economic performance of the energy systems, the associated environmental signature was neglected. It is important to consider environmental impact as part of the design objectives rather than as additional constraints on operation of the process designs [11-13]. In their literature review, Cano-Ruiz and McRae [11] concluded that the inclusion of environmental concerns as an objective function could lead to the discovery of design alternatives that improve both environmental and economic performance. In energy systems, a life cycle analysis (LCA) procedure is commonly used to evaluate the environmental impact of the system [14, 15]; the present work adopts such an LCA procedure to include the environmental impact as an additional objective function.

LCA is an objective process for evaluating the environmental burdens associated with a product, process or activity [16]. The first step in the application of LCA is identification and quantification of the energy and material used in a process, followed by estimation of the waste released to the environment associated with the energy use and material processing. This information is further translated into a set of environmental impacts that can be aggregated into different groups. These impacts are finally used to assess the absorption cycle design alternatives that may be implemented to achieve a reduction in environmental impact.

Even though LCA has been used as a tool to estimate and compare the environmental impacts of the design alternatives, it lacks a systematic means of generating design alternatives for environmental impact reductions. This shortcoming of LCA can be alleviated by combining it with optimization tools. Used in combination, the optimization tools generate design alternatives systematically and help a selection of the best choices according to the criterion included in the model while LCA helps to assess the design alternatives from an environmental perspective. Such a combination is widely recommended for process design optimization [12, 13], but has only been implemented in energy systems in a few cases [17-19].

To the authors' knowledge, the optimal design of single-effect water/LiBr absorption cycles that incorporates an environmental performance measure in the framework of multi-objective optimization is not yet available in the literature. The objective of the current work is to fill this research gap by combining mathematical programming with LCA principles.

This approach enables the systematic generation of absorption cycle design alternatives and environmental assessments that lead to designs with significant environmental benefits and a decreased chiller area requirement. The environmental performance is quantified using the global warming potential metric. Based on Eco-indicator 99 which follows LCA principles [20], the performance with respect to each impact and damage category for each optimal alternative design is also evaluated subsequent to the optimization. The optimal trade-off designs are obtained by implementing the epsilon constraint method [21]. The capabilities of the proposed approach are illustrated through a case study of the typical design of a single-effect water/LiBr absorption cycle.

2. Problem statement

Depending on the temperature level of the generator, absorption cycle's configuration can be half-effect, single-effect or multiple-effects [22, 23]. In this work, the single-effect water/Lithium Bromide absorption cycle is used;water is used as the refrigerant and LiBr as the absorbent.

Figure 1 depicts a schematic diagram of an absorption cycle on pressure-temperature coordinates; the system provides chilled water for cooling applications. The main components of the absorption cycle are the absorber (A), condenser (C), desorber (D), evaporator (E), refrigerant expansion valve (RV), solution heat exchanger (SHX), solution pump (P), and solution expansion valve (SV). The high-pressure units include the condenser, desorber and solution heat exchanger, while the low-pressure units are the absorber and evaporator. Following the stream numbering in Figure 1, the vapor refrigerant (stream 10) coming from the evaporator is absorbed by the strong solution stream (6). The resulting solution that leaves the absorber (stream 1) is weak in LiBr concentration. The heat of the solution released in the absorber is removed by the cooling water (stream 13 to 14). The weak solution is then pumped to a higher pressure by the solution pump. Stream 2 is preheated in the solution heat exchanger by recovering heat from the strong solution (stream 4) coming from the desorber. In the desorber, the refrigerant is boiled off by adding heat to the desorber (stream 11 to 12). Subsequently, the vapor (stream 7) goes to the condenser for complete condensation (stream 8) using the cooling water (stream 15 to 16). The liquid refrigerant (stream 8) flows to the evaporator through the refrigerant expansion valve to provide the cooling demand of the cycle by absorbing heat from the chilled water (stream 17 to 18). The strong liquid solution (stream 4) from the desorber returns to the absorber through the solution heat exchanger and the

solution expansion valve. The desorber heat demand is supplied by a gas-fired water heater. The gas-fired heater uses natural gas as its primary energy resource.

The problem addressed in this work can be formally stated as follows. The cooling capacity of the chiller, the inlet and outlet temperatures of the external fluids, the overall heat transfer coefficients of the heat exchangers, and life cycle inventory of emissions associated with the operation of the cooling system are given. The goal is to determine the optimal design and associated operating conditions that minimize simultaneously the total area of the chiller and its environmental impact.

3. Mathematical formulation

The design problem formulation builds on the work of Chavez-Islas and Heard [8], which focused only on the economic performance of ammonia/water absorption cycle, and of Gebreslassie et al. [10]. In the latter, a single-effect ammonia/water absorption cycle was used to provide chilled water at temperatures as high as 5^0C. However, for this type of application, a water/LiBr solution-supported chiller is superior in its simplicity during the desorption process, the overall performance, and in its capability to be driven at lower temperature [24]. Therefore, the problem formulation in the current work is focused on the design of a single-effect water/LiBr absorption cycle. Furthermore, the model is extended to include an exergy analysis of the cycle as well as the global warming potential as a measure of the environmental impact. The model is posed as a bi-criteria NLP problem that seeks to minimize the total area of the chiller and the environmental impact associated with the design. The resulting formulation relies on the following assumptions:

- Steady-state operation.
- Heat losses are not considered.
- Pressure losses are not considered.
- Constant overall heat transfer coefficients.
- The refrigerant leaving the condenser is saturated liquid.
- The weak and strong solutions leave the absorber and desorber, respectively, as saturated liquids.
- The temperature of the vapor leaving the desorber is at the equilibrium temperature of the solution concentration entering the desorber.

The equations involved in the mathematical formulation are grouped into four sets of constraints for (i) mass balance; (ii) energy balance including performance criteria; (iii) exergy balance; and (iv) the objective function. These are described next.

3. 1. Mass balance

Each process component can be treated as a control volume with its inlet and outlet streams. Mass conservation must be satisfied in each component of the chiller [4, 23] (Figure 2):

$$\sum_{j \in IN(k)} m_j z_{i,j} - \sum_{j \in OUT(k)} m_j z_{i,j} = 0 \qquad \forall k, s \tag{1}$$

Eqn. (1) represents the mass balances applied to each component k of the chiller and ensures that the amounts of substance i (water, LiBr) that enter component k equal the total amount of i leaving k. In this equation, m_j denotes the mass flow of stream j, and $z_{i,j}$ is the mass fraction of substance i in stream j; j can be either an inlet or outlet stream. Furthermore, IN(k) denotes the set of inlet streams to unit k, whereas OUT(k) includes all outlet streams.

3. 2. Energy balance

The energy balance applied to each component k of the chiller states that the difference in energy content between the inlet and outlet streams, plus the heat supplied to the component (Q_k^{IN}), must equal the heat removed (Q_k^{OUT}) plus the work done (W_k) by the component [4, 23] :

$$\sum_{j \in IN(k)} m_j h_j - \sum_{j \in OUT(k)} m_j h_j + Q_k^{IN} - Q_k^{OUT} - W_k = 0 \quad \forall k \tag{2}$$

The heat and work terms in Eqn. (2) can take a zero value in some of the components, as shown below:

$$Q_k^{IN} = 0 \;\; If \;\; k = \left\{ \begin{array}{l} Absorber\,(A) \\ Condenser\,(C) \\ Solution heat\, exchanger\;\; (SHX) \\ Pump(P) \\ Expansion valves(RV, SV) \end{array} \right\} \tag{3}$$

$$Q_k^{OUT} = 0 \;\; If \;\; k = \left\{ \begin{array}{l} Evaporator(E) \\ Desorber\,(D) \\ Solution\,heat\,exchanger\;(SHX) \\ Pump(P) \\ Expansion\,valves(RV,SV) \end{array} \right\} \tag{4}$$

$$W_k = 0 \qquad \forall k \neg pump \tag{5}$$

3. 3. Exergy balance

The exergy balance constraint ensures that the sum of the exergy difference between the entering and exiting streams and the exergy loss due to the heat transfer with the surrounding equals the work and the irreversibility rate (exergy destruction rate $\dot{I}_k$) of the component [4, 25]:

$$\sum_{j \in IN\,(k)} \dot{E}_j - \sum_{j \in OUT\,(k)} \dot{E}_j + Q_k^{IN}\left(1 - \frac{T_0}{T_k}\right) - Q_k^{OUT}\left(1 - \frac{T_0}{T_k}\right) - W_k - \dot{I}_k = 0 \qquad \forall k \tag{6}$$

In Eqn. (6) T_0 is the ambient temperature and T_k is the temperature at which component k transfers heat with the environment at constant temperature. For some of the components the exergy from heat transfer and work take zero values:

$$Q_k^{IN}\left(1 - \frac{T_0}{T_k}\right) = 0 \;\; if \;\; k = \left\{ \begin{array}{l} Absorber\,(A) \\ Condenser\,(C) \\ Solution heat\,exchanger\,(SHX) \\ Pump(P) \\ Expansion valves(RV, SV) \end{array} \right\} \tag{7}$$

$$Q_k^{OUT}\left(1 - \frac{T_0}{Tk}\right) = 0 \;\; if \;\; k = \left\{ \begin{array}{l} Evaporator(E) \\ Desorber\,(D) \\ Solution\,heat\,exchanger(SHX) \\ Pump(P) \\ Expansion\,valves(RV, SV) \end{array} \right\} \tag{8}$$

$$W_k = 0 \qquad \forall k \neg pump \tag{9}$$

where the exergy rate of stream j ($\dot{E}_j$) is determined as a function of the specific exergy of the stream (e_j) as:

$$\dot{E}_j = m_j e_j \qquad \forall j \tag{10}$$

If the entering and exiting components are the same, the chemical exergy of components cancels out in the exergy balance [4]. Hence, the specific exergy of the stream j (e_j) is determined from the physical exergy of the stream as:

$$e_j = (h_j - h_0) - T_0(s_j - s_0) \qquad \forall j \tag{11}$$

where h_j and s_j are specific enthalpy and entropy of stream j. The properties indicated by the subscript 0 refer to the ambient state, which is assumed as 25^0C and 1 bar ambient temperature and pressure, respectively.

Separate functions from Patek et al. [26, 27] are used to determine the thermodynamic properties of steam and the water/LiBr solution. The thermodynamic properties of steam are valid from 273 to 523 K. The correlations for the solution thermodynamics are valid for the full range of the composition and temperature range of 273 to 500 K.

3. 4. Performance indicators

The equations included in this section provide information about the absorption cycle performance based on the first law of thermodynamics and the exergy analysis. If these performance indicators are not considered as objective functions, it is possible to determine them once the model is solved (i.e., post-optimal analysis of the design solutions).

The coefficient of performance (*COP*) is defined as the ratio between the cooling capacity of the chiller and the energy supplied to the system [23] and is determined as follows:

$$COP = \frac{Q_{k=E}}{Q_{k=D} + W_{k=P}} \tag{12}$$

The exergetic efficiency (Ψ) is defined as the ratio between the exergy output and the exergy input to the chiller, that is, the ratio between the exergy output from the evaporator ($\dot{E}_{k=E}$) and the sum of the exergy inputs to the desorber ($\dot{E}_{k=D}$) and the pump ($W_{k=P}$) of the chiller, as:

$$\Psi = \frac{\dot{E}_{k=E}}{\dot{E}_{k=D} + W_{k=P}} \tag{13}$$

The circulation ratio (*f*) is defined as the ratio between the weak solution mass flow rate entering the desorber and the refrigerant vapor mass flow rate leaving the desorber. Depending on the mass fraction, it can be defined also as the ratio between the concentration gradient of the exiting streams and the strong and weak solution concentration gradient.

$$f = \frac{m_1}{m_7} = \frac{z_{LiBr,4}}{z_{LiBr,4} - z_{LiBr,3}} \tag{14}$$

4. Objective functions

The optimization model includes two conflicting objective functions: The total chiller area and the potential life cycle environmental impact.

4.1 Total area of the chiller

The total chiller area (A_t) given by the sum of each heat exchanger area (A_k) is determined as follows:

$$A_t = \sum_k A_k \qquad k = A, C, E, D \text{ and } SHX \tag{15}$$

The heat exchangers are modeled using the logarithmic mean temperature difference (ΔT_k^{lm}), the heat transfer area (A_k) and the overall heat transfer coefficient (U_k), as:

$$Q_k = U_k A_k \Delta T_k^{lm} \qquad k = A, C, E, D \text{ and } SHX \tag{16}$$

The numerical performance of the heat exchanger model is improved by employing Chen's approximation [28] to determine the logarithmic mean temperature difference (lmtd) of the heat exchanger. Chen's approximation is given as a function of the hot and cold end temperature differences (ΔT_k^h and ΔT_k^c, respectively) as shown in the following equation:

$$\Delta T_k^{lm} \cong \left[\Delta T_k^h \Delta T_k^c \frac{\Delta T_k^h + \Delta T_k^c}{2} \right]^{1/3} \qquad k = A, C, E, D \text{ and } SHX \tag{17}$$

4.2 Environmental performance of the chiller

As mentioned earlier, the environmental impact is quantified following LCA principles, as successfully adapted in process design applications [12, 13]. The calculation of the life cycle impact of the single-effect water/LiBr absorption cycle follows the four LCA steps [16]: (1) goal and scope definition; (2) inventory analysis; (3) impact assessment; and (4) interpretation.

4.2.1 Goal and scope definition

The system boundaries, the functional unit, and the life cycle impact assessment (LCIA) methodology are defined in this first step. LCA analysis is performed so as to include the generation of heat and electricity consumed by the absorption cycle. The environmental impact during the chiller construction is assumed to be negligible compared to that during operation [29]. The functional unit is the cooling capacity of the chiller. The environmental impact is evaluated based on the midpoint and endpoint approaches. In the midpoint approach, the environmental impact is quantified by means of the global warming potential (GWP). The GWP is calculated over a specific time interval that must be stated beforehand [30]. The IPCC 2007 framework considered a time horizon of 100 years as part of the Kyoto Protocol [30]. For the endpoint approach, Eco-indicator 99 is used.

4.2.2 Inventory analysis

This second step quantifies and analyzes the inventory of input/output data associated with the operation of the absorption cycle. The inventories are further translated to emissions (i.e., environmental burdens) represented by a continuous variable (LCI_b), which includes the emissions due to the extraction and combustion of natural gas, generation of the cooling water, and electricity, and is determined as follows:

$$LCI_b = \sum_t nT_{op} \left(Q_{k=D} LCIE_b^{heat} + m_{cw} LCIE_b^{cw} + W_{k=P} LCIE_b^{elec} \right) \tag{18}$$

In this equation, T_{op} and n are the annual operation hours and life span in years of the absorption cycle, respectively. Parameters $LCIE_b^{heat}$, $LCIE_b^{cw}$ and $LCIE_b^{elec}$ denote the life

cycle inventory of emissions of chemical b contributing to the environmental burden per unit of reference flow (*i.e.*, heat, amount of cooling water and electricity, respectively). These values, which can be retrieved from an environmental database [31], depend on the particular features of the absorption cycle (*e.g.*, type of primary energy source used in the heater, electricity mix of the country in which the cycle operates, etc.). Finally, the continuous variables Q_D, m_{cw} and W_k denote the heat demand of the chiller, cooling water mass flow rate, and electricity consumption of the pump, respectively.

4.2.3 Impact assessment

In this life cycle impact assessment step, the inventory of emissions is translated into the corresponding contributions to the impact, according to the following two approaches.

Midpoint approach: the global warming potential is determined as:

$$GWP = \sum_b LCI_b \, \phi_b \tag{19}$$

Parameter ϕ_b is a damage factor that accounts for the global warming potential of chemical b relative to that of CO_2, as published by the IPCC [32]. However, it should be noted that environmental databases such as Ecoinvent [31] provide both the life cycle inventory of emissions as well as the associated environmental impacts per functional unit. In such a case, Eqn. (19) may be omitted, as the GWP per the reference flow values (GWP_{heat}, GWP_{cw} and GWP_{elec}) is directly available in the database. The total GWP is then determined as follows:

$$\mathrm{G}WP = \sum_{\mathrm{t}} nT_{op} \, (\mathrm{Q}_{\mathrm{k=D}} \mathrm{G}WP_{heat} + m_{cw} \mathrm{G}WP_{cw} + W_{\mathrm{k=P}} \mathrm{G}WP_{elec}) \tag{20}$$

Endpoint approach: The impacts in each impact category, the damage model, and the total Eco-indicator 99 are estimated according to Eco-indicator 99 [20] as follows. First, the damage in each impact category is calculated from the life cycle emissions inventory and the impact model:

$$IMC_c = \sum_b LCI_b df_{bc} \qquad \forall c \tag{21}$$

In this model, IMC_c denotes the damage caused in impact category c, and df_{bc} is the coefficient of the damage model associated with chemical b and impact category *c*. The

damage factors link the results of the inventory phase and the damage in each impact category.

The second step is to aggregate impact categories into their corresponding damage category (d). This gives the impact in each damage category (DMC_d) as:

$$DMC_D = \sum_{j \in ID(d)} IMC_c \qquad \forall d \tag{22}$$

where ID*(*d*)* represents the set of impact categories included in the damage category d.

The last step is to translate the impact of the damage categories into the single total Eco-indicator 99 (ECO_{99}) metric:

$$ECO_{99} = \sum_d nf_d wf_d DAM_d \qquad \forall d \tag{23}$$

where nf_d and wf_d are normalization and weighting factors, respectively. The values of these parameters depend on the following three cultural perspectives [31]: Hierarchist damage model and normalization with average weighting, Egalitarian damage model and normalization with Egalitarian weighting, and Individualist damage model and normalization with Individualist weighting.

4.2.4 Interpretation

The interpretation phase entails an analysis of the optimal trade-off solutions for the multi-objective optimization problem. Post-optimal analysis of the Pareto design alternatives helps the decision-maker to choose the most suitable one which minimizes environmental impact at a marginal increase in the absorption cycle total area.

5. Solution method

If only environmental criteria are used as the objective function to be optimized, the design would be ideal from an environmental point of view but may not be economically competitive. Conversely, considering only the total chiller area could lead to an economically attractive design but one that does not satisfy environmental impact considerations. A truly optimal trade-off design needs a simultaneous consideration of these two objective functions. The design task is therefore formulated as a bi-criteria nonlinear programming (NLP) problem

(M) that simultaneously minimizes the total chiller area ($A_t(x)$) and the global warming potential (GWP(x)) associated with the operation of the chiller:

$$\begin{aligned} (M) \quad & \min_{x} \quad U(x) = \{A_t(x), GWP(x)\} \\ & s.t. \quad h(x) = 0 \\ & \quad\quad g(x) \leq 0 \\ & \quad\quad x \in \Re \end{aligned} \tag{24}$$

In this formulation, *x* denotes the design variables (*i.e.*, thermodynamic properties, flows, operating conditions, and sizes of equipment units). The equality constraints h(x) = 0 represent thermodynamic property relations, mass, energy and exergy balances constraints, heat exchanger area, and LCA calculations, as laid out in Eqn. (1) to Eqn. (23). The inequality constraint $g(x) \leq 0$ is added to model design specifications such as capacity limits and bounds on process variables.

The solution to this optimization problem (M) is given by a set of efficient or Pareto optimal points representing a unique combination of the chiller total area and the environmental impact. To obtain the Pareto designs, the ε - constraint method [10, 21] is implemented.

6. Case study

The absorption cycle described in Section 2 with a 100 kW cooling capacity is optimized assuming a life span of 20 years and 5040 operating hours per year. The cycle is driven by low-grade heat and utilizes water/LiBr as the working fluid pair. The operating conditions, heat exchanger design parameters and environmental data for the problem are given in Table 1 and Table 2.

The global warming potential (GWP_{heat}) associated with the generation and combustion of natural gas in the gas-fired heater, 0.076279 $kgCO_{2\text{-}eq}$ per MJ of heat, is retrieved from Eco invent [31]. This term accounts for the emissions during the fuel generation, construction of the boiler, direct emissions during combustion, and electricity consumed for boiler operation.

The normalization and weighting factors, parameters used to aggregate the damage models into the single Eco-indicator 99 metric, depend on the chosen cultural perspective and weightings. In the present work, the Average Hierarchist perspective [20] is used. According

to this perspective, human health and ecosystem qualities are assumed to be equally important with a weighting of 40% each, and the resource depletion contributes the remaining 20% of the damage score. The human health damage normalization factor is 1.52×10^{-2}, while for ecosystem damage, it is 5.13×10^{3}, and for resource depletion, 8.41×10^{3} [20].

6.1 Pareto optimal set of designs

The NLP optimization model of the single-effect water/LiBr absorption cycle is implemented in the Generic Algebraic Modeling System (GAMS) optimization environment [33]. The model is solved with CONOPT [34] NLP solver. The resulting optimization problem includes 380 constraints and 361 variables. Pareto optimal designs are obtained in about 3 seconds of computational time each. Since solutions from such a solver are dependent on a good initial guess, the same problem is simulated in Engineering Equation Solver (EES) [35] and the results are used as initial guesses for the optimization problem in GAMS.

First, by optimizing each scalar objective function, the lower ($\underline{\epsilon}$) and upper ($\overline{\varepsilon}$) limits of the search interval within which all ε fall are determined. The next step is partitioning the interval $\left[\underline{\epsilon}, \overline{\varepsilon}\right]$ into 20 equal sub-intervals. Finally, using the model MA each limit of the sub-intervals is calculated.

Figure 3 presents Pareto optimal solutions of the chiller designs obtained following the solution method explained in Section 5 and the previous paragraph. Only the thermodynamic properties of the extreme designs: the minimum chiller area design (Table 3) and the minimum environmental impact design (Table 4) are presented along with one optimal trade-off design (Table 5).

Each Pareto optimal design represents a unique combination (trade-off) between the total chiller area and global warming potential operating under specific conditions. As shown in Figure 3, the global warming potential is decreased along the Pareto curve at the expense of increasing the total chiller area. This can be explained by the fact that as the heat exchanger areas of the chiller increase, the energy consumption of the chiller decreases. The global warming potential is directly proportional to the heat consumption of the chiller as shown in Eqn. (20). Along the Pareto frontier, the two objectives cannot be improved simultaneously; the performance improvement of one objective function is obtained only at the expense of deterioration in performance of the second objective function. This can be illustrated using the

Pareto optimal design point B shown in Figure 3. The global warming potential (GWP) is reduced by 21.6% by increasing the chiller area from 35.4 to 53 m2. In the other direction, the chiller area is reduced by 65.3% by increasing the GWP by 4%. The results show that instead of selecting the extreme designs, an optimal trade-off design with important performance improvement in one of the objective functions, without significant deterioration of a second objective function, can be identified from the Pareto set.

Figure 4 shows the coefficient of performance (COP) and exergetic efficiency (Ψ) of the chiller as a function of the chiller area for the entire Pareto frontier. It may be noted that once the COP and Ψ approach their maximum values (0.78 and 0.253, respectively), there is little performance improvement even as the chiller area is increased significantly past a certain value. This result is confirmed by evaluating the Pareto curve shown in Figure 3. Once the GWP reaches 3960 tonCO2-eq, the reduction in the GWP is negligible even at the expense of significantly increasing the chiller area.

6.2 Extreme Pareto optimal solutions

Extreme Pareto optimal designs are those at the minimum total surface area (design A in Figure 3) and the minimum global warming potential design (design C in Figure 3). The thermodynamic properties for each flow stream of these designs are given in Table 3 and Table 4, and include temperature, pressure, LiBr concentration, specific enthalpy, entropy and exergy of each state point. In the same tables, the mass flow rate of each stream is also presented. As can be seen from Table 3, the concentration difference between the strong and weak solutions ($z_{LiBr,4}$ - $z_{LiBr,3}$) in the solution circuit is reduced because of the minimum area available for absorption and desorption. To overcome the effect of a reduction in refrigerant flow rate and a reduction in cooling capacity, the solution circulation rate must increase in order to desorb more refrigerant. To heat the high solution flow rate, the heat demand of the desorber increases. On the contrary, for the minimum global warming potential design (Table 4), the chiller area is at a maximum. At this maximum area, the absorption and desorption processes are enhanced, and the concentration difference between the strong and weak solution increases. In this case, the circulation rate decreases, leading to the minimum energy consumption and thus, less environmental impact.

6.2.1 Energy, exergy and environmental impact analysis

The energy balance results for the extreme designs and one random optimal trade-off design are presented in Figure 5. The results presented in this figure confirm that for the minimum chiller area design, the heat added to the desorber and the heat rejected from the absorber increase. This is due to the heat transfer area reduction in the absorption and desorption components. The converse is true for the minimum GWP design.

The performance indicators of the extreme designs and one optimal trade-off design are presented in Table 6. The table includes the coefficient of performance (COP), exergetic efficiency (Ψ), circulation ratio (f), concentration difference between the strong and weak solutions (ΔZ), chiller area (A_t), global warming potential (GWP) considering the life cycle greenhouse gas emissions, and global warming potential (GWP_{CO_2}) considering only the carbon dioxide emissions from combustion of the natural gas. The strong and weak solution concentration difference decreases and the solution circulation rate increases along the Pareto curve in the direction of minimum global warming design to the minimum chiller area design. Therefore, the heat demand and exergy destruction increase along the curve. This leads to a decrease in the COP and exergetic efficiency, as shown in Table 6. It may be noted that the results show a 27.8% difference between the GWP considering the life cycle greenhouse gas emissions and that considering only the carbon dioxide emissions from the combustion of natural gas. Therefore, to evaluate the environmental performance of thermal systems, the life cycle emissions inventory entries must be considered.

Figure 6 depicts the contribution of each damage category (human health, ecosystem quality and natural resource depletion) to the total Eco-indicator 99 of the extreme designs and one Pareto optimal design. To reduce the environmental impact by 24.7% within the extreme designs, the chiller surface area must increase by a factor of 4.3. This is not economically attractive because the investment cost increases proportionally with the chiller area. However, when utilizing the optimal trade-off solutions, an important reduction in environmental impact may be achieved without significantly compromising the chiller area. For instance, as explained in Section 6.2, the choice of Design B in Figure 3 results in an improvement in the environmental performance by 21.6% at the expense of an increase in the chiller area by 33%.

Figure 6 also shows that 87% of the total Eco-indicator 99 comes from natural resource depletion while a 12% contribution is from the human health damage (which includes climate

change as one of its impact categories). This implies that the environmental impact due to natural resource depletion dominates the total impact, and should not be overlooked in assessing the environmental performance of thermal systems.

6.3 Evaluation for different operating conditions

The absorption cycle optimization model results are dependent on the operating parameters of the cycle. To illustrate this variation, the model is optimized for values of the operating parameters that are different from the base case (in Table 1). Results of minimum global warming and minimum chiller area designs are presented below as functions of the temperatures of the generator, cooling water and chilled water.

6.3.1 Generator temperature

Figure 7 and Figure 8 show the effect of the generator temperature on the minimum chiller area design and minimum GWP designs, respectively. In general, the following effects are observed as the generator temperature increases:

- As the desorption process temperature increases, the generation of water vapor is enhanced and the strong solution concentration increases and the concentration gradient between the strong and weak solution increases. As a result, the circulation ratio decreases per Eqn. (14). This leads to a decrease in the heat load of the generator, and consequently a decrease in the GWP.
- In the solution heat exchanger, the weak solution heat gain increases. The heat load in the absorber and generator decreases, and the GWP decreases.
- The temperatures of the working fluids exiting from the generator increase, resulting in an increase in the average temperatures of both the absorber and condenser. This results in an increase in exergy destruction in the absorber and condenser and reduces the performance of the cycle. In this case, the heat demand and the GWP increase.
- The temperature difference between the incoming weak solution stream and the heating medium of the generator increases. This effect leads to an increase in exergy destruction in the generator. As a result, the heat loads of the generator and the environmental impact increase.

For the minimum chiller area design, at low temperatures, the first two effects dominate the third and fourth, and a reduction in the chiller area and the environmental impact can be

obtained. However, beyond 110^0C, the third and fourth effects become significant, and the heat demand of the chiller as well as the global warming potential increase (Figure 7).

The minimum GWP design, which corresponds to the maximum chiller area, is obtained at the minimum generator temperature (Figure 8). As the generator temperature increases, the first two positive effects become dominant. The minimum global warming potential is not reduced because the minimum possible GWP is obtained at the minimum generator temperature. But this effect is until the generator temperature reaches 115^0C; in this range, as the generator temperature increases, the chiller area decreases. Beyond 115^0C, the third and fourth effects become significant and the energy consumption increases to overcome the increase in exergy destruction and consequently the GWP increases.

As the generator temperature increases from 115^0C to 120^0C, the condenser exit temperature increases from 30.2^0C to 32.55^0C, which results in an increase in condenser lmtd from 0.94^0C to 3.7^0C. Because the objective is to minimize the GWP, the increase in heat demand is not significant. Moreover, the overall heat transfer coefficient is assumed constant (as discussed in Section 3). Therefore, according to Eqn. (16), the condenser area is reduced proportionally with its lmtd increase (see the sudden drop in chiller area in Figure 8).

6.3.2 Cooling water temperature

The effects of cooling water temperature on the chiller model optimization results are discussed next.

In the condenser, as the cooling water temperature increases, the high pressure of the cycle increases [23]. This leads to a decrease in the concentration of the strong solution, and a corresponding reduction in the concentration gradient ($z_{LiBr,4}$ - $z_{LiBr,3}$) between the strong and weak solutions. Since the circulation ratio increases per Eqn. (14), the thermal load of the absorber and generator increases. The GWP also increases per Eqn. (20). As shown in Table 7 and Table 8, for the minimum global warming potential design, the increase in environmental impact because of the cooling temperature increase is not as significant as for the minimum chiller area design. This is because of the compensating effect of the significant increase in the heat exchanger areas, which contributes to a lowering of the environmental impact.

In the absorber, as the cooling water temperature increases, the weak solution concentration ($z_{LiBr,1} = z_{LiBr,3}$) increases [23] because the rate of absorption of the water vapor decreases. This results in a decrease in the gradient between the strong and weak solutions and a consequent increase in circulation rate. Because the solution flow rate increases in the absorber and desorber, the thermal load of the absorber and generator increases as well, as shown in Table 7 and Table 8.

6.3.3 Chilled water temperature

With an increase in the evaporator temperature, the low pressure of the cycle increases and the weak solution concentration decreases [23]. This results in an increase in concentration gradient between the strong and weak solutions, and a decrease in the circulation rate. The heat removed from the absorber and the heat demand of the desorber both decrease. As a result, the heat exchanger areas decrease. Because of the proportional relationship between the environmental impact and the heating demand, the GWP decreases. This effect can be seen from the results presented in Table 9 and Table 10.

7. Conclusions

A systematic method for reducing the life cycle environmental impact of absorption cooling cycles is developed. The method formulates a bi-criteria nonlinear programming (NLP) problem that identifies designs that minimize the total chiller area and the environmental impact of the absorption system. The environmental impact is evaluated according to life cycle assessment (LCA) principles.

The optimal design of a typical single-effect water/LiBr absorption cooling cycle is discussed. Significant reductions in the total area of the chiller designs are shown at a marginal increase in environmental impact. The methodology presented in this work is intended to promote a more sustainable design of absorption cooling systems by guiding decision makers towards the adoption of alternatives that result in lower environmental impact.

The effects of the generator, cooling water and chilled water temperatures on the minimum global warming potential and minimum chiller area designs are explored using the model developed. The results show that an increase in the generator temperature improves the performance of the chiller at low generator temperatures and hence improves the

environmental impact performance and reduces the chiller area. As the generator temperature increases further, the increase in performance levels off due to the exergy destruction increase in the absorber, condenser and generator that results from the increase in temperature difference between the internal and external fluid temperatures of the units.

Supplementary material available on the journal website provides tabulated values of the thermodynamic properties and heat exchanger (HX) minimum temperature approaches, lmtd, area, heat, exergy input, exergy output and exergy destruction for each Pareto set of designs.

Nomenclature

Indices

b	Chemical emissions
c	Impact category
d	Damage category
i	Component of a stream
j	Streams
k	Component

Sets

ID (d)	Set of impact categories included in the damage category *d*
IN(k)	Set of input streams to component *k*
OUT(k)	Set of output streams from component *k*

Parameters

ϕ_b	Global warming potential of chemical b with respect to CO_2 [$kgCO_{2\text{-}eq}$ /kg]
df_{bc}	Damage factor associated with chemical b and impact category c [impact/kg]
GWP_{cw}	Life cycle global warming potential per kg of cooling water [$kgCO_{2\text{-}eq}$ /kg]
GWP_{elec}	Life cycle global warming potential per kW of electricity [$kgCO_{2\text{-}eq}$ /kW]
GWP_{heat}	Life cycle global warming potential per kWh of heat [$kgCO_{2\text{-}eq}$ /kWh]
$LCIE^{cw}{}_b$	Life cycle inventory entry of chemical b per kg of cooling water [kg /kg]
$LCIE^{elec}{}_b$	Life cycle inventory entry of chemical b per kW of electricity [$kgCO_{2\text{-}eq}$ /kW]
$LCIE_b{}^{heat}$	Life cycle inventory entry of chemical b per kWh of heat [kg/kWh]
n	Life span of the chiller [years]
nf_d	Normalization factor [Eco-Indicator-99 points /impact]
T_{op}	Operational hours [h/yr]

U_k	Overall heat transfer co-efficient of heat exchanger k [kW/m^2/K]
wf_d	Weighting factor [-]

Variables

A_k	Area of heat exchanger k [m^2]
A_t	Total area of the chiller [m^2]
COP	Coefficient of performance [-]
DMC_d	Damage in category d [impact]
ECO_{99}	Environmental impact in Eco-Indicator 99 [points]
e_j	Specific exergy of stream j [kJ/kg]
E_j	Exergy rate of stream j [kW]
f	Circulation ratio [kg/kg]
GWP	Global warming potential of the chiller during its life span [ton$CO_{2\text{-}eq}$]
h_j	Specific enthalpy of stream j [kJ/kg]
IMC_c	Damage in impact category c [impact]
LCI_b	Life cycle inventory entry associated with chemical b [kg]
m_j	Mass flow rate of stream j [kg/s]
m_{cw}	Mass flow rate of cooling water j [kg/s]
P_j	Pressure of stream j [bar]
Q_k	Heat transferred in component k [kW]
Q^k_{IN}	Heat input to component k [kW]
Q_k^{OUT}	Heat output from component k [kW]
s_j	Specific entropy of stream j [kJ/kgK]
T_j	Temperature of stream j [^{o}C or K]
W_k	Mechanical power of pump [kW]
$z_{i,j}$	Mass fraction of substance i in stream j [-]
ΔT^k_{lm}	Logarithmic mean temperature difference [K]
ΔT^k_h	Temperature difference in the hot end [K]
ΔT^k_c	Temperature difference in the cold end [K]
ψ	Exergetic efficiency of the chiller [-]

References

[1] Allali A, Bojariu R, Diaz S, Elgizouli I, Griggs D, Hawkins D, et al. Climate Change 2007: Synthesis Report. 2007.
[2] IEA. How the energy sector can deliver on a climate agreement in Copenhagen. International Energy Agency; 2009.
[3] KizIlkan Ö, Sencan A, Kalogirou SA. Thermoeconomic optimization of a LiBr absorption refrigeration system. Chemical Engineering and Processing: Process Intensification. 2007;46:1376-84.
[4] Kotas TJ. The exergy method of thermal plant analysis: Krieger Pub Co; 1995.
[5] Gebreslassie BH, Medrano M, Mendes F, Boer D. Optimum heat exchanger area estimation using coefficients of structural bonds: Application to an absorption chiller. International Journal of Refrigeration. 2010;33:529-37.
[6] Biegler LT, Grossmann IE. Retrospective on optimization. Computers & Chemical Engineering. 2004;28:1169-92.
[7] Grossmann IE, Biegler LT. Part II. Future perspective on optimization. Computers & Chemical Engineering. 2004;28:1193-218.
[8] Chavez-Islas ML, Heard CL. Design and Analysis of an Ammonia/Water Absorption Refrigeration Cycle by Means of an Equation-Oriented Method. Industrial & Engineering Chemistry Research. 2009;48:1944-56.
[9] Chavez-Islas ML, Heard CL, Grossmann IE. Synthesis and Optimization of an Ammonia-Water Absorption Refrigeration Cycle Considering Different Types of Heat Exchangers by Application of Mixed-Integer Nonlinear Programming. Industrial & Engineering Chemistry Research. 2009;48:2972-90.
[10] Gebreslassie BH, Guillén-Gosálbez G, Jiménez L, Boer D. Design of environmentally conscious absorption cooling systems via multi-objective optimization and life cycle assessment. Applied Energy. 2009;86:1712-22.
[11] Cano-Ruiz JA, McRae GJ. Environmentally conscious chemical process design. Annual Review of Energy and the Environment. 1998;23:499-536.
[12] Hugo A, Pistikopoulos EN. Environmentally conscious long-range planning and design of supply chain networks. Journal of Cleaner Production. 2005;13:1471-91.
[13] Guillen-Gosalbez G, Antonio Caballero J, Jimenez L. Application of life cycle assessment to the structural optimization of process flowsheets. Industrial & Engineering Chemistry Research. 2008;47:777-89.
[14] Fleck B, Huot M. Comparative life-cycle assessment of a small wind turbine for residential off-grid use. Renewable Energy. 2009;34:2688-96.
[15] Cherubini F. GHG balances of bioenergy systems - Overview of key steps in the production chain and methodological concerns. Renewable Energy. 2010;35:1565-73.
[16] IRAM-ISO-14040. Environmental management-Life Cycle Assessment-Principles and frame work. International Standard: ISO Standards; 2006.
[17] Bernier E, Maréchal F, Samson R. Multi-objective design optimization of a natural gas-combined cycle with carbon dioxide capture in a life cycle perspective. Energy. 2010;35:1121-8.
[18] Ren H, Zhou W, Nakagami Ki, Gao W, Wu Q. Multi-objective optimization for the operation of distributed energy systems considering economic and environmental aspects. Applied Energy. 2010;87:3642-51.
[19] Lazzaretto A, Toffolo A. Energy, economy and environment as objectives in multi-criterion optimization of thermal systems design. Energy. 2004;29:1139-57.

[20] PRé-Consultants. The Eco-indicator 99, A damage oriented method for life cycle impact assessment. Methodology report and manual for designers. Amersfoort, The Netherlands: PRé-Consultants; 2000.
[21] Ehrgott M. Multicriteria Optimization2000.
[22] Gebreslassie BH, Medrano M, Boer D. Exergy analysis of multi-effect water-LiBr absorption systems: From half to triple effect. Renewable Energy. 2010;35:1773-82.
[23] Herold K, Radermacher R, SA K. Absorption chillers and heat pumps. Boca Raton, Florida: CRC Press; 1996.
[24] Kalogirou SA. Solar thermal collectors and applications. Progress in Energy and Combustion Science. 2004;30:231-95.
[25] Sencan A, Yakut KA, Kalogirou SA. Exergy analysis of lithium bromide/water absorption systems. Renewable Energy. 2005;30:645-57.
[26] Pátek J, Klomfar J. A computationally effective formulation of the thermodynamic properties of LiBr-H_2O solutions from 273 to 500 K over full composition range. International Journal of Refrigeration. 2006;29:566-78.
[27] Pátek J, Klomfar J. A simple formulation for thermodynamic properties of steam from 273 to 523 K, explicit in temperature and pressure. International Journal of Refrigeration. 2009;32:1123-5.
[28] Thomas F Edgar, David M. Himmelblau, Lasdon LS. Optimization of chemical processes: McGraw-Hill; 2001.
[29] Gebreslassie BH, Guillén-Gosálbez G, Jiménez L, Boer D. A systematic tool for the minimization of the life cycle impact of solar assisted absorption cooling systems. Energy. 2010;35:3849-62.
[30] Plattner Gian-Kasper, Thomas Stocker, Pauline Midgley, Tignor. M. IPCC Expert Meeting on the Science of Alternative Metrics. 2009.
[31] Jungbluth N, Sonnenkollektor-Anlagen. Ecoinvent report No. 6-XI. Dübendorf, CH: Swiss Centre for Life Cycle Inventories; 2007.
[32] Solomon S, Qin D, M. Manning, Chen Z, Marquis M, Averyt KB, et al. Contribution of working group i to the fourth assessment report of the intergovernmental panel on climate change. Technical report. 2007.
[33] Brooke A, Kendrik D, Meeraus A, Raman R, Rosenthal. RE. GAMS - A User's Guide. GAMS Development Corporation. Washington1998.
[34] Drud A. CONOPT Solver Manual. ARKI Consulting and Development. Bagsvaerd, Denmark1996.
[35] F-Chart Software, Engineering Equation Solver (EES).

List of Tables

Table 1 Process data of the absorption cooling cycle.

Heat transfer coefficients *U [kW/m²K]*	
Absorber	0.7
Condenser	2.5
Evaporator	1.5
Desorber	1.5
Solution heat exchanger	1
Temperature data [°C]	
Chilled water inlet/outlet	11.2/7
Condenser cooling water inlet/outlet	27.4/30
Absorber cooling water	27.4/30
Generator hot water temperature	90/85
Other data	
Cooling capacity [kW]	100
Mass transfer effectiveness	0.9
Pump efficiency	0.6

Table 2 Environmental data associated with producing hot water per MJ of heat.

	Impact Category	**Unit**	**Heat**
1.	Carcinogens	DALY	3.76×10^{-6}
2.	Climate change	DALY	3.8427×10^{-4}
3.	Ionizing radiation	DALY	4.14×10^{-7}
4.	Ozone layer depletion	DALY	2.37×10^{-7}
5.	Respiratory effects	DALY	1.5864×10^{-4}
6.	Acidification & eutrophication	PDF·$m^2 \cdot yr$	2.07×10^{-5}
7.	Ecotoxicity	PDF·$m^2 \cdot yr$	3.94×10^{-6}
8.	Land occupation	PDF·$m^2 \cdot yr$	1.63×10^{-5}
9.	Fossil fuels	MJ surplus	3.913×10^{-3}
10.	Mineral extraction	MJ surplus	2.2×10^{-6}

Table 3 Minimum chiller area design thermodynamic properties at each flow stream for design A of Figure 3.

Stream	**T[^0C]**	**P[kPa]**	**m[kg/s]**	**z[kg/kg]**	**h[kJ/kg]**	**s[kg/kg/K]**	**e[kJ/kg]**
1	35.4	0.65	0.797	0.583	97.8	0.2	42.3
2	35.4	5.87	0.797	0.583	97.8	0.51	-49.9
3	52.9	5.87	0.797	0.583	131.8	0.31	44.3
4	84.6	5.87	0.754	0.616	213	0.46	79.2
5	65.4	5.87	0.754	0.616	177.2	0.9	-86
6	65.4	0.65	0.754	0.616	177.2	0.36	74.1
7	75.8	5.87	0.043	0	2642	8.57	92
8	35.8	5.87	0.043	0	150	0.52	0.88
9	0.8	0.65	0.043	0	150	0.01	150.9
10	0.8	0.65	0.043	0	2502	9.13	-216.2
11	90	100	8.01	0	376.9	1.19	26.3
12	85	100	8.01	0	355.9	1.13	22.7
13	27.4	100	14.89	0	115	0.4	0.06
14	30	100	14.89	0	125.9	0.44	0.21
15	27.4	100	9.74	0	115	0.4	0.06
16	30	100	9.74	0	125.9	0.44	0.21
17	11.2	100	5.67	0	47.1	0.17	1.3
18	7	100	5.67	0	29.4	0.11	2.3

Table 4 Minimum environmental impact design thermodynamic properties at each flow stream for design C of Figure 3.

Stream	**T[^0C]**	**P[kPa]**	**m[kg/s]**	**z[kg/kg]**	**h[kJ/kg]**	**s[kg/kg/K]**	**e[kJ/kg]**
1	27.6	0.99	0.225	0.512	56.3	0.2	2.3
2	27.6	4.3	0.225	0.512	56.3	0.4	-59.5
3	50.1	4.3	0.225	0.512	104.5	0.35	3.7
4	83.1	4.3	0.183	0.629	223.8	0.44	96.3
5	50	4.3	0.183	0.629	164.5	0.7	-40.6
6	50	0.99	0.183	0.629	164.5	0.27	89.2
7	53.9	4.3	0.042	0	2600.9	8.59	44.2
8	30.2	4.3	0.042	0	126.7	0.44	0.23
9	6.8	0.99	0.042	0	126.7	0.1	100.5
10	6.8	0.99	0.042	0	2513.1	8.98	-159.2
11	90	100	6.026	0	376.9	1.19	26.3
12	85	100	6.026	0	355.9	1.13	22.7
13	27.4	100	11.28	0	115	0.4	0.06
14	30	100	11.28	0	125.9	0.44	0.21
15	27.4	100	9.53	0	114.97	0.4	0.06
16	30	100	9.53	0	125.85	0.44	0.21
17	11.2	100	5.67	0	47.06	0.17	1.3
18	7	100	5.67	0	29.41	0.11	2.3

Table 5 Chiller thermodynamic properties for optimal trade-off design B of Figure 3.

Stream	T[^0C]	P[kPa]	m[kg/s]	z[kg/kg]	h[kJ/kg]	s[kg/kg/K]	e[kJ/kg]
1	31.1	0.86	0.316	0.542	70.9	0.2	16.6
2	31.1	5.17	0.316	0.542	70.9	0.45	-59.3
3	58.1	5.17	0.316	0.542	126.4	0.37	19.4
4	85.3	5.17	0.274	0.626	223.3	0.46	91.1
5	50	5.17	0.274	0.626	159.2	0.7	-46
6	50	0.86	0.274	0.626	159.2	0.27	83.2
7	63.6	5.17	0.042	0	2619.2	8.56	71.6
8	33.5	5.17	0.042	0	140.4	0.48	0.56
9	4.9	0.86	0.042	0	140.4	0.07	122.9
10	4.9	0.86	0.042	0	2509.6	9.03	-177.3
11	90	0	6.278	0	376.9	1.19	26.3
12	85	0	6.278	0	355.9	1.13	22.7
13	27.4	0	11.68	0	115	0.4	0.06
14	30	0	11.68	0	126	0.44	0.21
15	27.4	0	9.61	0	115	0.4	0.06
16	30	0	9.61	0	125.9	0.44	0.21
17	11.2	0	5.67	0	47	0.17	1.31
18	7	0	5.67	0	29.4	0.11	2.3

Table 6 Performance indicators of the extreme designs and one representative optimal trade-off design (Designs A, B and C from Figure 3).

	COP [-]	Ψ [-]	ΔZ [kg⁄kg]	f [kg⁄kg]	A_t m^2	GWP [ton$CO_{2\text{-eq}}$]	GWP_{CO2} [tonCO_2]
Min(A_t)	0.595	0.193	0.033	18.7	35.4	5167	3726
Pareto(B)	0.759	0.246	0.084	7.5	53.0	4051	2921
Min(GWP)	0.791	0.256	0.117	5.4	153	3889	2804

Table 7 Minimum global warming potential design performance indicators as a function of cooling water temperature ($T_{13}(T_{14})$= (inlet(exit)).

$T_{13}(T_{14})[^0C]$	COP[-]	Ψ[-]	ΔZ	f[kg/kg]	$A[m^2]$	$GWP[tonCO_{2\text{-}eq}]$
25/28	0.803	0.254	0.123	5.0	143.9	3830
27/30	0.791	0.250	0.117	5.4	152.5	3889
30/33	0.778	0.246	0.111	5.8	158.5	3955
32/35	0.770	0.243	0.105	6.1	179.0	3998

Table 8 Minimum chiller area design performance indicators as a function of cooling water temperature ($T_{13}(T_{14})$= (inlet(exit)).

$T_{13}(T_{14})= [^0C]$	COP[-]	Ψ[-]	ΔZ	f[kg/kg]	$A[m^2]$	$GWP[tonCO_{2\text{-}eq}]$
25/28	0.612	0.193	0.037	16.8	31	5027
27/30	0.597	0.189	0.034	18.3	34.1	5152
30/33	0.581	0.184	0.031	20.1	39.1	5292
32/35	0.567	0.179	0.028	21.8	43.9	5428

Table 9 Minimum global warming potential design performance indicators as a function of chilled water temperature (T_{17} (T_{18})).

$T_{17}(T_{18})[^0C]$	COP[-]	Ψ[-]	ΔZ	f[kg/kg]	$A[m^2]$	$GWP[tonCO_{2\text{-}eq}]$
5/9.2	0.777	0.280	0.12	5.4	150.9	3956
7/11.2	0.792	0.250	0.118	5.3	148.6	3883
9/13.2	0.808	0.220	0.118	5.2	146.9	3807

Table 10 Minimum chiller area design performance indicators as a function of chilled water temperature ($T_{17}(T_{18})$).

$T_{17}(T_{18})[^0C]$	COP[-]	Ψ[-]	ΔZ	f[kg/kg]	$A[m^2]$	$GWP[tonCO_{2\text{-}eq}]$
5/9.2	0.598	0.215	0.034	18.1	36.2	5139
7/11.2	0.599	0.189	0.034	18.1	33.7	5138
9/13.2	0.607	0.166	0.035	17.4	31.9	5065

List of Figures

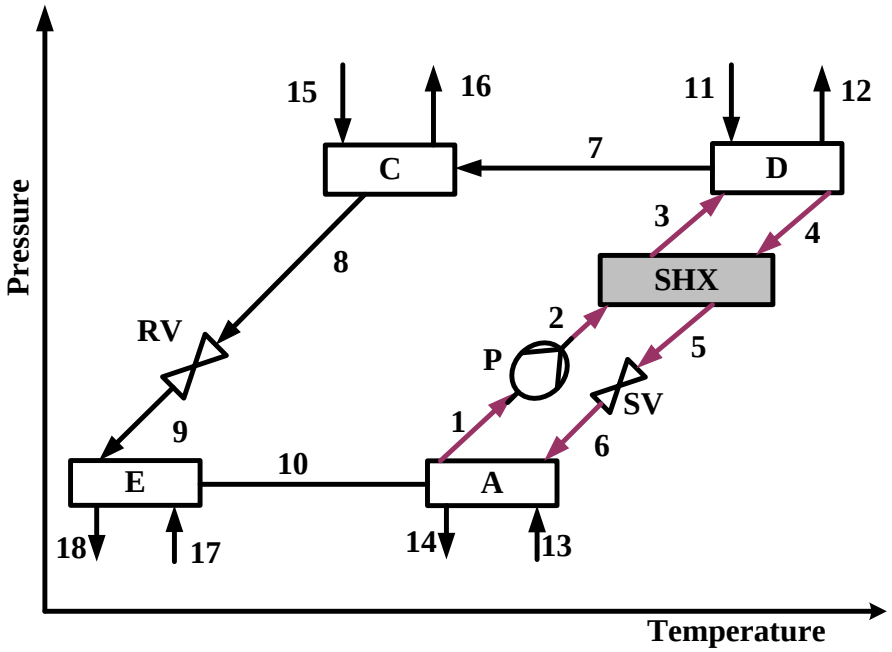

Figure 9 Single-effect Water/LiBr absorption cycle with inlets and outlets.

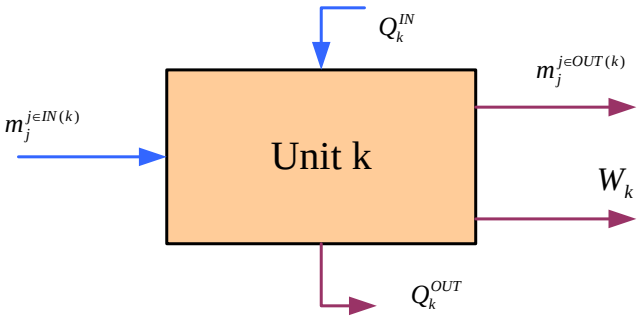

Figure 10 A generic unit of the absorption cycle with its inlets and outlets.

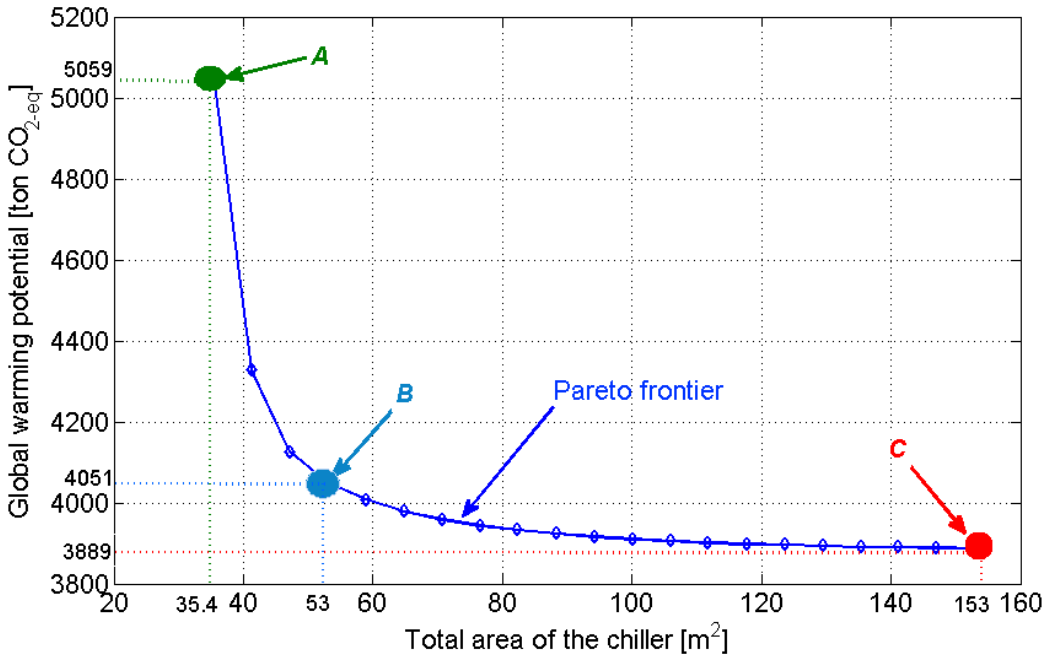

Figure 11 Pareto set of absorption cycle designs of the case study.

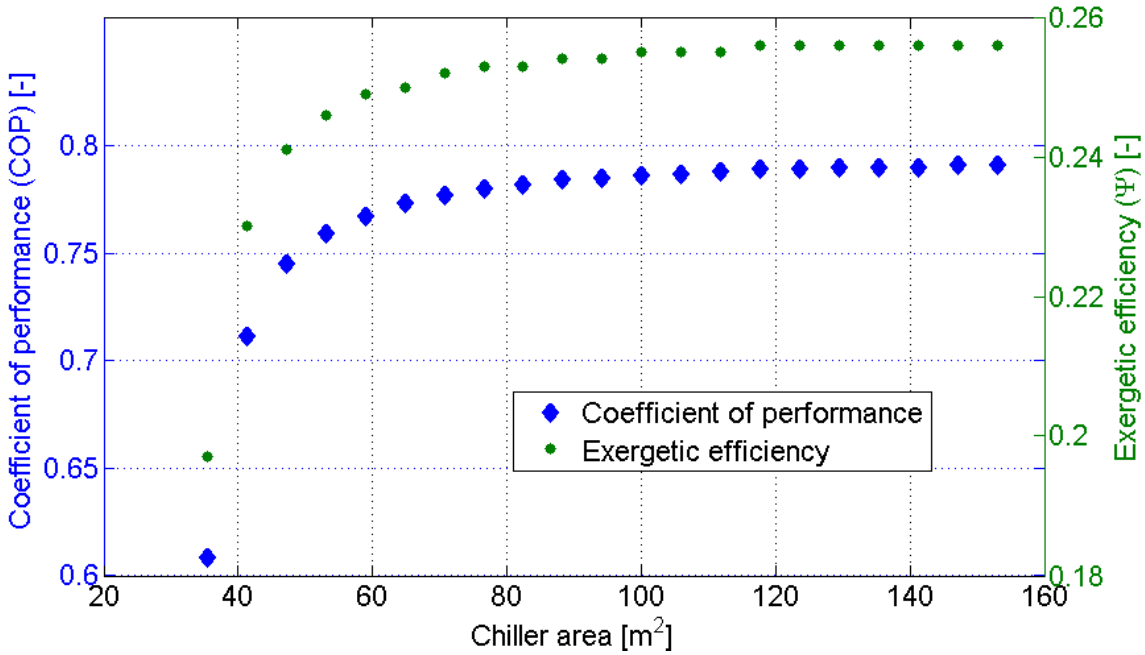

Figure 12 Coefficient of performance and exergetic efficiency of the Pareto frontiers as a function of the chiller area.

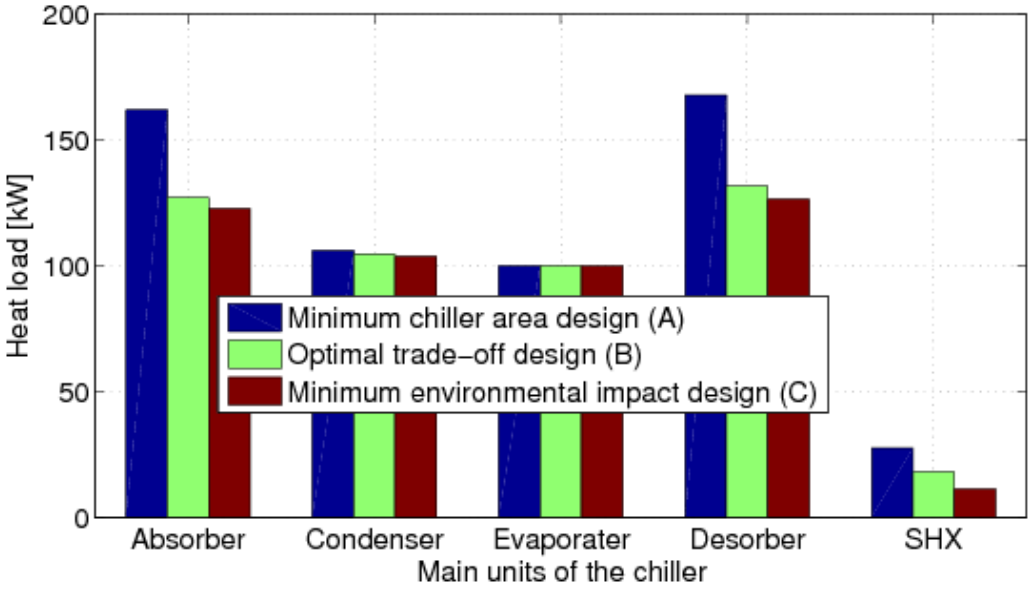

Figure 13 Energy analysis of the selected optimal designs.

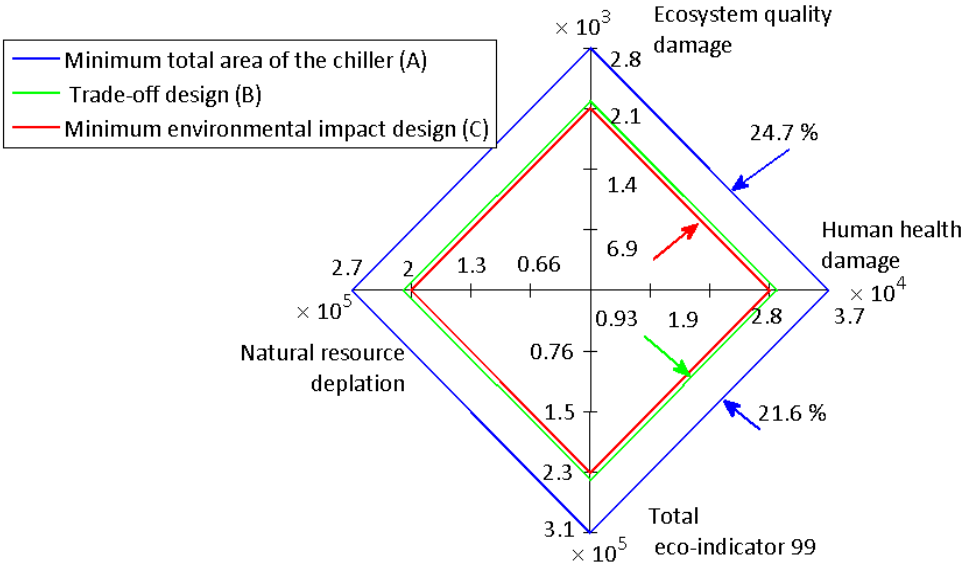

Figure 14 Eco-indicator 99 of the total and each damage categories for the extreme designs and a representative trade-off design.

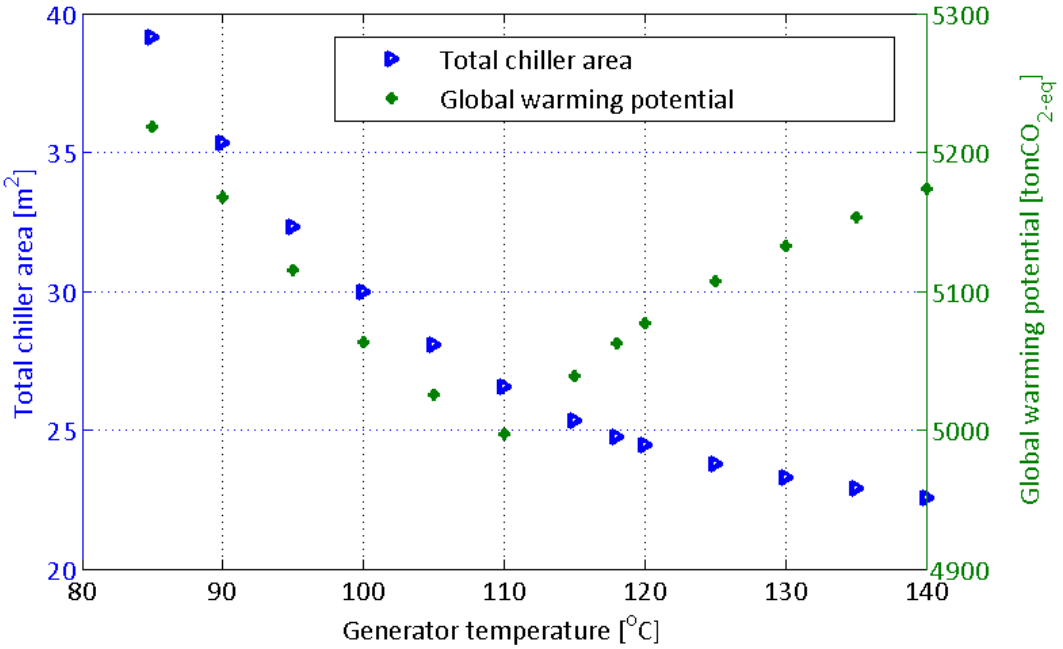

Figure 15 Minimum chiller area designs as a function of generator temperature.

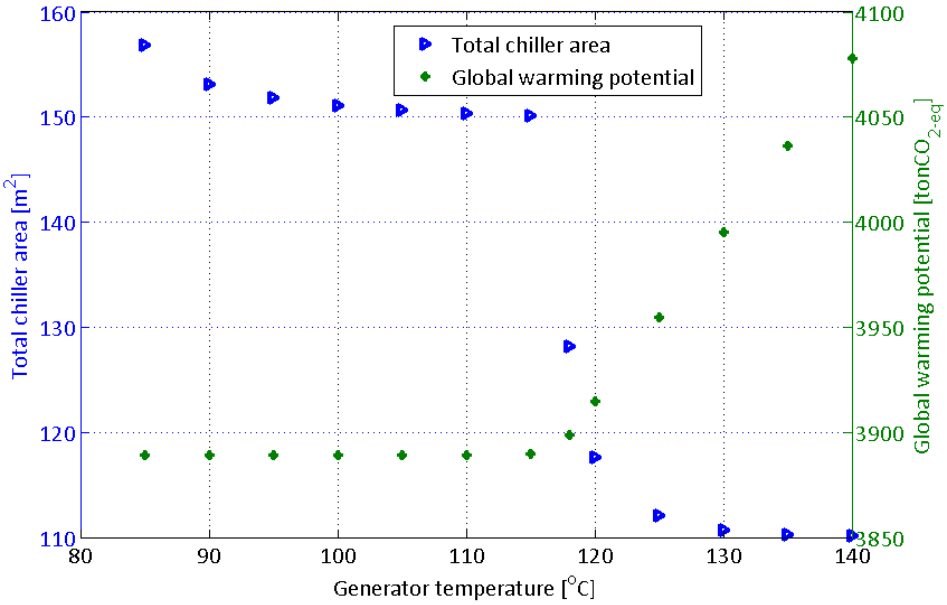

Figure 16 Minimum global warming potential designs as a function of generator temperature.